Published in final edited form as:
Biochem Pharmacol. 2007 May 1; 73(9): 1499–1510. doi:10.1016/j.bcp.2007.01.010.

Effects of hydroxyl radical scavenging on cisplatin-induced p53 activation, tubular cell apoptosis and nephrotoxicity

Man Jiang[a,1], **Qingqing Wei**[a], **Navjotsin Pabla**[a], **Guie Dong**[a], **Cong-Yi Wang**[b], **Tianxin Yang**[c], **Sylvia B. Smith**[a], and **Zheng Dong**[a,*]

[a]Department of Cellular Biology and Anatomy, Medical College of Georgia and Veterans Affairs Medical Center, 1459 Laney Walker Blvd., Augusta, GA 30912, United States

[b]Center for Genomic Medicine, Medical College of Georgia and Veterans Affairs Medical Center, 1459 Laney Walker Blvd., Augusta, GA 30912, United States

[c]Department of Internal Medicine, University of Utah and Veterans Affairs Medical Center, Salt Lake City, UT 84148, United States

Abstract

Nephrotoxicity is a major side effect of cisplatin, a widely used cancer therapy drug. Recent work has suggested a role of p53 in renal cell injury by cisplatin. However, the mechanism of p53 activation by cisplatin is unclear. This study determined the possible involvement of oxidative stress in p53 activation under the pathological condition using *in vitro* and *in vivo* models. In cultured renal proximal tubular cells, cisplatin at 20 μM induced an early p53 phosphorylation followed by protein accumulation. Cisplatin also induced reactive oxygen species (ROS), among which hydroxyl radicals showed a rapid and drastic accumulation. Dimethylthiourea (DMTU) and *N*-acetyl-cysteine (NAC) attenuated hydroxyl radical accumulation, and importantly, diminished p53 activation during cisplatin treatment. This was accompanied by the suppression of PUMA-α, a p53-regulated apoptotic gene. Concomitantly, mitochondrial cytochrome crelease and apoptosis were ameliorated. Notably, DMTU and NAC, when added post-cisplatin treatment, were also inhibitory to p53 activation and apoptosis. In C57BL/6 mice, cisplatin at 30 mg/kg induced p53 phosphorylation and protein accumulation, which was also abrogated by DMTU. DMTU also ameliorated tissue damage, tubular cell apoptosis and cisplatin-induced renal failure. Collectively, this study has suggested a role of oxidative stress, particularly hydroxyl radicals, in cisplatin-induced p53 activation, tubular cell apoptosis and nephrotoxicity.

Keywords

Cisplatin; Nephrotoxicity; Apoptosis; p53; Hydroxyl radical; Oxidative stress

1. Introduction

Cisplatin is a widely used chemotherapy drug for cancers [1,2]. Major side effects of cisplatin include nephrotoxicity, leading to acute kidney injury and renal failure [3,4]. Under the pathological condition, cisplatin activates multiple signaling pathways, resulting in necrosis

*Corresponding author. Tel.: +1 706 721 2825; fax: +1 706 721 6120. E-mail address: E-mail: zdong@mail.mcg.edu (Z. Dong).
[1]Exchange graduate student at Medical College of Georgia, as part of the International Cooperative Agreement between Medical College of Georgia and Wuhan University School of Medicine in China.

and apoptosis of renal tubular cells [5–18]. However, it is unclear how the signals are integrated to determine tubular cell injury and death [3,4].

Recent work has suggested a role of p53 in cisplatin-induced tubular cell apoptosis [19,20]. p53 is activated during cisplatin treatment. Importantly, cisplatin-induced tubular cell apoptosis is attenuated by pifithrin-α, a pharmacological inhibitor of p53 [19,20]. A dominant-negative mutant of p53 abrogates cisplatin-induced apoptosis as well [20]. Mechanistically, p53 may promote apoptosis by inducing apoptotic genes such as caspases [21] and Bcl-2 family proteins like PUMA-α [22]. Despite these observations, the upstream signals leading to p53 activation during cisplatin nephrotoxicity remain unknown.

Oxidative stress via reactive oxygen species (ROS) has been implicated in renal injury under various pathological conditions [23,24]. Interestingly, ROS may participate in p53 regulation [25]. ROS induces DNA damage, which is a robust trigger of p53 activation. In addition, ROS can activate an array of signaling pathways involving various protein kinases to result in p53 phosphorylation and activation [25]. During cisplatin nephrotoxicity, oxidative stress mainly involving ROS is induced in renal tubular cells [4,23]. Importantly, amelioration of oxidative stress by a variety of ROS scavengers can protect the cells against cisplatin injury [6,26–31]. With this background, the current study has determined the possible involvement of oxidative stress in p53 activation during cisplatin-induced tubular cell apoptosis *in vitro* and cisplatin nephrotoxicity *in vivo*. Our results show that ROS, particularly hydroxyl radicals, accumulates rapidly following cisplatin treatment. Amelioration of hydroxyl radical accumulation by pharmacological scavengers diminishes p53 activation, which is accompanied by the suppression of tubular cell apoptosis, preservation of tissue histology, and protection of renal function.

2. Materials and methods

2.1. Materials

The rat kidney proximal tubular cell (RPTC) line was from Dr. U. Hopfer at Case Western Reserve University, and maintained for cisplatin incubation as previously [20,22]. Antibodies were from the following sources: polyclonal anti-p53 and antiphospho-p53 (Serine 15) antibodies from Cell Signaling Technology (Beverly, MA); monoclonal anti-Bax (1D1) from NeoMarkers (Fremont, CA); monoclonal anti-cytochrome *c* from BD Sciences Pharmingen (San Diego, CA); polyclonal anti-PUMA from Dr. J. Yu at University of Pittsburgh; secondary antibodies from Jackson ImmunoResearch (West Grove, PA). For the measurement of hydroxyl radicals, 2-thiobarbituric acid, trichloroacetic acid and 2-deoxy-D-ribose were purchased from Fisher Chemicals (Fair Lawn, NJ). For the measurement of ROS, 2′,7′-dichlorodihydrofluorescein diacetate (H_2DCFDA) was purchased from Molecular Probes (Eugene, OR). Other reagents were purchased from Sigma (St. Louis, MO).

2.2. Cisplatin incubation of RPTC cells

RPTC cells were treated with cisplatin in two ways. First, as described in our recent publications [20,22], cells at ~90% confluence were incubated with 20 μM cisplatin for 16 h. To test the effects of various inhibitors or ROS scavengers, the agents were present along with cisplatin during the whole incubation period. Second, 20 μM cisplatin was added to the cells for 2 h and then removed by three-time washes with PBS. ROS scavengers including dimethylthiourea (DMTU) and *N*-acetyl-cysteine (NAC) were added post-cisplatin treatment to test their effects. The second method of cisplatin treatment was specifically used in the experiment of Fig. 6, which was designed to avoid possible effects of ROS scavengers on cisplatin uptake.

2.3. Measurement of reactive oxygen species

Production of ROS was measured with the fluorogenic dye 2′,7′-dichlorodihydrofluorescein diacetate (H_2DCFDA), a cell-permeant compound. Cells were pre-incubated with 10 μM H_2DCFDA for 30 min at 37 °C. After the extracellular dye was removed, the cells were washed and incubated with cisplatin in Hanks' buffer for the indicated period of time. Subsequently, the fluorescence was measured at 485 nm excitation and 535 nm emission using a plate reader (GENios, Tecan US Inc., Research Triangle Park, NC).

2.4. Measurement of hydroxyl radicals

Hydroxyl radicals were measured by the deoxyribose degradation assay as described by Baliga et al. [6]. In this assay, 2-deoxyribose is cleaved in the presence of hydroxyl radicals to release a substance that reacts with thiobarbituric acid to produce a chromogen with absorbance at 532 nm [32]. Briefly, 2-deoxy-D-ribose at 3 mM was added to cells just prior to the addition of cisplatin. After incubation, 0.5 ml of medium was collected and mixed with 0.5 ml of 1% (w/v) 2-thiobarbituric acid in 50 mM NaOH and 0.5 ml of 2.8% (w/v) trichloroacetic acid. The mixture was then heated at 100 °C for 15 min, cooled, and extracted with *n*-butanol. The supernatant was measured for absorbance at 532 nm. The amount of hydroxyl radicals was calculated by using the extinction coefficient of 156 mM^{-1} cm^{-1}, and expressed as nmol/mg protein.

2.5. Analysis of apoptosis

Apoptosis was routinely monitored by morphological methods and by the measurement of caspase activity [20,33]. For morphological assessment, cells were fixed with 4% paraformaldehyde and stained with Hoechst 33342. Cellular and nuclear morphologies were examined by phase contrast and fluorescence microscopy, respectively. Typical apoptotic cells showed cellular shrinkage, nuclear condensation and fragmentation, and formation of apoptotic bodies. Four fields with ~200 cells per field were examined in each dish to estimate the percentage of apoptosis. Images of representative fields were also recorded. For caspase measurement, an enzymatic assay was conducted [20,22,34]. Briefly, cell lysate extracted with 1% Triton X-100 was added to an enzymatic reaction containing 50 μM DEVDS·AFC, a fluorogenic caspase substrate. Fluorescence during the reaction was measured to calculate the caspase activity.

2.6. Flow cytometric assay of apoptosis

In addition to morphological examination, apoptosis was also quantified by flow cytometric analysis using the Annexin V-FITC Apoptosis Detection kit from BD PharMingen (San Diego, CA). After incubation, cells were detached from dishes by trypsinization and harvested along with the floating cells by centrifugation at 1000 × *g* for 5 min. Following washing in PBS containing 2% BSA, the cells were resuspended in binding buffer (10 mM Hepes–NaOH, 140 mM NaCl, 2.5 mM $CaCl_2$) at a final density of (1–2) × 10^6 cells/ml. Hundred microlitres of single cell suspension was incubated with 5 μl Annexin V-FITC and 5 μl propidium iodide (PI) for 15 min at room temperature in the dark. After adding 400 μl of binding buffer, the samples were analyzed by using a BD FACSCalibur flow cytometer (BD Biosciences, San Jose, CA) within 1 h. For each sample, 10,000 events were counted.

2.7. Cellular fractionation

Cells were fractionated into cytosolic and membrane-bound organellar fractions as previously [33–36]. Briefly, 0.05% digitonin in an isotonic buffer (in mM: 250 sucrose, 10 Hepes, 10 KCl, 1.5 $MgCl_2$,1 EDTA and 1 EGTA; pH 7.1) was added to the cells for 2–5 min of extraction at room temperature. Subsequently, the cells were harvested by scraping and centrifuged to collect the supernatants as cytosolic fraction. The remaining digitonin insoluble part was

dissolved in 2% SDS buffer as the membrane-bound organellar fraction containing mitochondria. The fractions were analyzed by immunoblot analysis using standard procedure.

2.8. Cisplatin-induced nephrotoxicity in C57 mice

C57BL/6 mice (male, 8–10 weeks, Jackson Laboratory) were administered with a single dose of cisplatin (i.p., 30 mg/kg) to induce nephrotoxicity [37]. To test the effects of DMTU, 100 mg/kg DMTU was administered 30 min prior to cisplatin injection, and then daily post-cisplatin treatment as described by Ramesh and Reeves [28]. For control animals, vehicle solution was administered. Renal function was monitored by measuring serum creatinine and blood urea nitrogen (BUN), as detailed in our recent work [37,38].

2.9. Examination of histology, apoptosis, p53 in renal tissues

To examine renal histology, renal tissues were fixed with 4% paraformaldehyde, embedded in paraffin and sectioned at 4 μm for hematoxylin/eosin staining [37–39]. Apoptosis in renal tissues was analyzed by TUNEL assay using a kit from Roche applied sciences (Indianapolis, IN), as described in our previous work [33,37,38]. Briefly, deparaffinized tissue sections were exposed to terminal transferase (TdT) in the presence of a nucleotide mixture containing fluorescein-12-dUTP and examined by fluorescence microscopy. To examine p53 by immunofluorescence, tissue sections were exposed to specific antibodies against p53 or phospho-p53. After extensive wash, the tissue sections were stained with Cy3-conjugated secondary antibodies for fluorescence microscopy.

2.10. Statistical analysis

Data were expressed as mean ± S.D. ($n \geq 3$). Statistical analysis was conducted using the GraphPad Prism software. Statistical differences in multiple groups were determined by multiple comparisons with Tukey's post-tests following analysis of variance. Statistical differences between two groups were determined by Student's *t*-test. $P < 0.05$ was considered statistically significant.

3. Results

3.1. Early p53 activation following cisplatin treatment

Our previous work has characterized an *in vitro* model of cisplatin nephrotoxicity, resulting in tubular cell apoptosis. In this model, we have demonstrated p53 activation prior to the development of apoptosis [20,22]. To examine the signals that were involved in p53 activation, we determined the earliest time points of p53 activation during cisplatin treatment. p53 activation was indicated by the accumulation and phosphorylation of the protein. Representative blots are shown in Fig. 1A, and the results of densitometric analysis are summarized in Fig. 1B and C. Statistically significant p53 accumulation was detected after 4 h of cisplatin treatment, which was 1.5-fold over control (Fig. 1A, lane 6 and Fig. 1B). On the contrary, p53 phosphorylation was detected much earlier (Fig. 1A and C). Densitometry of blots from separate experiments showed that significant p53 phosphorylation occurred after 30 min of cisplatin treatment. By 1 h, phosphorylated p53 (p-p53) was ~2.4-fold over control and increased further during longer cisplatin incubation (Fig. 1A and C). As an internal control, the expression of β-actin did not change during the period of examination. Consistent with our previous results [20], p53 activation was shown mainly in the nucleus (not shown). Together, the results demonstrate a rapid p53 phosphorylation during cisplatin treatment, which was followed by p53 accumulation. These observations are consistent with the general understanding of p53 regulation, where post-translational modifications particularly phosphorylation may stabilize this protein and induce its accumulation [40,41].

3.2. Rapid hydroxyl radical accumulation following cisplatin treatment

The early p53 phosphorylation shown in Fig. 1 suggests that the signal(s) for p53 activation must be very rapid in response to cisplatin treatment. To identify the signal(s), we initially focused on reactive oxygen species (ROS), which have been implicated in cisplatin nephrotoxicity [6,27]. Intracellular ROS accumulation was measured using DCF, which became fluorescent after being oxidized. As shown in Fig. 2A, there was a consistent increase of ROS within the cells upon cisplatin incubation. ROS accumulation was detected after 1 h of cisplatin, and the accumulation was maintained during prolonged cisplatin treatment (Fig. 2A). ROS includes a variety of partially reduced metabolites of oxygen such as superoxide, hydrogen peroxide, and hydroxyl radicals. Among them, hydroxyl radicals are considered one of the most reactive and potent oxidant. Of much relevance to our study, hydroxyl radicals have been suggested to be the most important ROS mediating cisplatin nephrotoxicity [6,26–28]. To determine the role of hydroxyl radicals in p53 activation, we initially examined hydroxyl radical accumulation following cisplatin treatment. Hydroxyl radicals were measured by the deoxyribose degradation assay, which was used in early studies to examine hydroxyl radical accumulation during cisplatin treatment of renal tubular cells [6]. The results are shown in Fig. 2B. Clearly, hydroxyl radicals showed a striking increase upon cisplatin exposure, which was over 10 times higher than control. Importantly, the accumulation was rapid, reaching a maximal level within 15 min (Fig. 2B). Thereafter the high level of hydroxyl radicals was sustained during the measurement period of 4 h. Apparently, hydroxyl radicals accumulated rapidly following cisplatin treatment, preceding p53 phosphorylation and activation.

3.3. Effects of ROS scavengers on p53 activation during cisplatin treatment

To directly examine the role of hydroxyl radicals in p53 activation, we tested the effects of antioxidants and ROS scavengers. The chemicals were added along with cisplatin for 16 h of incubation. Consistent with our previous work [20], cisplatin elicited a noticeable p53 accumulation and phosphorylation, which was ameliorated by pifithrin-α, a pharmacological inhibitor of p53 (Fig. 3A, lanes 2 and 3). *N*-Acetyl-cysteine (NAC), a general antioxidant, suppressed p53 induction as well as phosphorylation (lane 4). Similar inhibitory effects were shown for DMTU, a specific hydroxyl radical scavenger (lane 5). In contrast, no inhibitory effects were shown for Tiron and catalase, respective scavengers of superoxide and hydrogen peroxide (lane 6 and data not shown). The results of densitometric analysis of several experiments are shown in Fig. 3B and C, further confirming the inhibitory effects of NAC and DMTU on cisplatin-induced p53 activation. Of note, these chemicals do not affect cisplatin accumulation in cells [30].

To verify the scavenging effects of NAC and DMTU on hydroxyl radicals, we determined hydroxyl radical accumulation during cisplatin treatment (Fig. 3D). Consistent with earlier results shown in Fig. 2, cisplatin stimulated a rapid and marked increase of hydroxyl radicals. Within 1 h of cisplatin incubation, hydroxyl radicals increased from <0.1 to 0.81 nmol/mg protein. The increase was reduced to 0.34 nmol/ mg protein by NAC. DMTU also suppressed hydroxyl radical accumulation. As expected, Tiron did not scavenge hydroxyl radicals under the experimental condition (Fig. 3D).

3.4. Effects of hydroxyl radical scavengers on cisplatin-induced tubular cell apoptosis

The results described above have suggested that hydroxyl radicals contribute to p53 activation during cisplatin treatment. Considering the recent evidence for a role of p53 in cisplatin injury [19–22], it was hypothesized that hydroxyl radical scavengers including DMTU might ameliorate tubular cell apoptosis under our experimental condition. To test this possibility, we initially examined the development of apoptosis by morphological approaches. As shown in Fig. 4A, cisplatin treatment for 16 h led to apoptotic morphology in many cells (images in the middle). These cells assumed a condensed configuration with typical apoptotic bodies. The

nuclei of these cells also became condensed and fragmented. Importantly, the development of apoptosis was suppressed by DMTU (images on the right side). By cell counting, cisplatin induced ~50% apoptosis (Fig. 4B). Consistent with previous work [20,22], pifithrin-α inhibited p53 activation and suppressed apoptosis. Importantly, NAC and DMTU suppressed apoptosis to 12 and 14%, respectively. In sharp contrast, no inhibitory effects were shown for Tiron (Fig. 4B), which did not scavenge hydroxyl radicals and did not attenuate p53 activation (Fig. 3). We further quantified apoptosis by flow cytometric analysis of Annexin V/PI staining. A representative analysis was shown in Fig. 4C. Consistent with the morphological assessment (Fig. 4B), 49.2% cells were Annexin V positive after cisplatin incubation (Fig. 4C). DMTU reduced Annexin V positive cells to 22.6%. To confirm the morphological observations, we also measured caspase activity. As shown in Fig. 4D, cisplatin stimulated caspase activation, which was suppressed by pifithrin-α, NAC and DMTU but not by Tiron. Thus, consistent with other studies [6,26–31], our results suggest the involvement of hydroxyl radicals in cisplatin-induced tubular cell injury. Of particular interest, hydroxyl radicals may contribute to p53 activation to initiate apoptosis.

3.5. Inhibition of PUMA-α induction and Bax/cytochrome c redistribution by DMTU during cisplatin treatment

Our recent work has demonstrated the regulation of PUMA-α by p53 during cisplatin treatment of renal tubular cells [22]. PUMA-α, a Bcl-2 family protein, is induced by p53 in mitochondria, wherein it interacts with and neutralizes Bcl-XL, leading to the activation of Bax, permeabilization of mitochondria followed by the release of cytochrome *c* and apoptosis [22]. To determine whether hydroxyl radicals participate in the activation of these mitochondrial events of apoptosis, we specifically examined the effects of DMTU. We first examined PUMA-α induction. As shown in Fig. 5A, PUMA-α was drastically induced during cisplatin treatment (lane 2), and the induction was completely blocked by DMTU (lane 3). We then examined Bax activation by analyzing its accumulation in mitochondria. As shown in Fig. 5B, the majority of Bax was detected in the cytosol of control cells (lane 1); following cisplatin incubation, Bax translocated into the mitochondrial fraction (lane 2). Importantly, Bax translocation during cisplatin treatment was suppressed by DMTU (Fig. 5B, lane 3). Finally, we analyzed the effects of DMTU on cytochrome *c* (cyt.c) release during cisplatin treatment. As shown in Fig. 5C, cyt.c was in mitochondria in control cells (lane 1), and was released into the cytosol following cisplatin treatment (lane 2). Cyt.c release during cisplatin treatment was attenuated by DMTU (lane 3). Collectively, the results suggest that DMTU, by scavenging hydroxyl radicals, may diminish p53 activation during cisplatin treatment, and as a result, attenuate PUMA-α induction and suppress the mitochondrial pathway of apoptosis.

3.6. DMTU and NAC, when added post-cisplatin treatment, can suppress p53 activation and apoptosis

The results presented above indicate that DMTU and NAC, when added along with cisplatin, can suppress p53 activation and tubular cell apoptosis. One possibility was that DMTU/ NAC might interfere with cisplatin uptake by the cells and, as a result, block its cytotoxic effects. To determine whether the inhibitory effects of DMTU/NAC were (in)dependent of cisplatin uptake, we tested the effects of DMTU/NAC added after cisplatin exposure. To this end, cisplatin was added to the cells for 2 h and was then completely removed. DMTU and NAC were added post-cisplatin treatment. As shown in Fig. 6A, DMTU and NAC, added after cisplatin treatment, suppressed apoptosis from 50 to 18 and 25%, respectively. The results were supported by the measurement of caspase activity (Fig. 6B). We further determined p53 activation under the experimental condition. As shown in Fig. 6C, p53 was phosphorylated and accumulated in response to 2 h of cisplatin exposure (lane 2). DMTU and NAC added after cisplatin incubation still ameliorated p53 activation (lanes 3 and 4). Together, the results suggest that DMTU and NAC can suppress p53 activation and tubular cell apoptosis without

affecting cisplatin uptake. This inference is supported by previous work showing that ROS scavengers including DMTU do not affect cisplatin uptake by renal tubular cells and renal tissues [31].

3.7. Inhibition of cisplatin nephrotoxicity and p53 activation in vivo by DMTU

To extend the *in vitro* findings to *in vivo* systems, we examined the effects of DMTU in a characterized mouse model of cisplatin nephrotoxicity [28,37]. In this model, a single dose of cisplatin-induced severe renal failure within 3 days. We measured serum creatinine and blood urea nitrogen (BUN), two common indicators of acute renal failure. As shown in Fig. 7, serum creatinine and BUN increased respectively to 2.15 and 164 mg/dl in cisplatin-treated animals, while the values remained low in the vehicle control group. Importantly, DMTU attenuated cisplatin-induced renal failure. As shown in Fig. 7A and B, serum creatinine and BUN were 0.64 and 73 mg/dl, respectively, in the cisplatin + DMTU group. The renoprotective effects of DMTU were further confirmed by the preservation of renal histology. As shown in Fig. 7C, cisplatin treatment induced obvious renal tissue damage including tubular dilation, lysis and cast formation. The tissue injury was partially prevented by DMTU. We also examined the effects of DMTU on cisplatin-induced tubular cell apoptosis by TUNEL staining (Fig. 7D). Clearly cisplatin led to the appearance of TUNEL positive cells, which again was suppressed by DMTU.

We further analyzed p53 activation during cisplatin nephrotoxicity and the effects of DMTU. As shown in Fig. 8A, both p53 and phospho-p53 were drastically induced by cisplatin (lanes 2 and 5), indicating p53 activation under the pathological condition. Notably, the activation was abrogated by DMTU (lanes 3 and 6). The immunoblot results were confirmed by immunofluorescence staining of renal tissues. As shown in Fig. 8B, p53 staining was minimal in control tissues, and was induced mainly in tubular cells following cisplatin treatment. Importantly, the number of p53 positive cells was significantly reduced in the tissues treated with cisplatin + DMTU. Similarly, we detected an increase of phospho-p53 immunofluorescence following cisplatin treatment, and again DMTU was inhibitory (not shown).

4. Discussion

Using *in vitro* and *in vivo* models, this study has suggested evidence for the involvement of oxidative stress in p53 activation during cisplatin-induced renal cell injury and nephrotoxicity. Hydroxyl radicals appear to be particularly relevant to p53 activation under the pathological condition. Following cisplatin treatment, hydroxyl radicals accumulate rapidly, correlating with early p53 phosphorylation and preceding p53 protein stabilization and induction. DMTU, a relatively specific hydroxyl radical scavenger, decreases hydroxyl radical accumulation and ameliorates p53 activation. Similar effects are shown for NAC, a general antioxidant. Non-hydroxyl radical scavengers (e.g. Tiron, catalase) do not prevent p53 activation during cisplatin treatment.

A pitfall of the use of ROS scavengers is the potential nonspecific effects of the chemicals. While this is an inherent technical issue of pharmacological studies, we have measured hydroxyl radicals during cisplatin treatment and determined the effects of various ROS scavengers. These measurements show different effects of the scavengers on hydroxyl radical accumulation during cisplatin treatment. Importantly, NAC and DMTU decrease hydroxyl radical accumulation, and only these two are effective in blocking p53 activation. Tiron and catalase, respective scavengers of superoxide and hydrogen peroxide, are without effects. These measurements suggest a correlation between hydroxyl radical accumulation and p53 activation. It is noteworthy that DMTU, a more specific hydroxyl radical scavenger, is less effective than NAC in scavenging hydroxyl radicals in our measurements. The results suggest

that the fraction of ROS that is inhibited by NAC, but not by DMTU, could be a different species of free radicals. However, inhibition of hydroxyl radical formation might be sufficient to prevent p53 activation.

In cultured renal tubular NRK52E cells, Tsuruya et al. have shown that DMTU does not interfere with cellular uptake of cisplatin [31]. Importantly, DMTU does not affect cisplatin incorporation in renal tissues after administration in animals [31]. Due to technical difficulties, cisplatin is not measured in the current study. Nevertheless, we show that DMTU and NAC, when added post-cisplatin incubation, can also suppress p53 activation and apoptosis (Fig. 6). Thus, these two scavenging chemicals can block cisplatin-induced signaling without affecting cisplatin uptake by the cells.

Although hydroxyl radicals may contribute to early p53 activation during cisplatin treatment, the underlying mechanism is unclear. After entering the cell, due to the decrease of chloride concentration, cisplatin is aquated, turning into highly reactive platinum species. These species may crosslink DNA and react with other nucleophiles such as glutathione, lipids and proteins, resulting in the disruption of cellular homeostasis followed by cell injury and death [2]. The current understanding of cisplatin cytotoxicity is mainly derived from the investigation of cancer cells. Apparently, in these cells the primary toxic effect of cisplatin is DNA damage via cross-linking and formation of DNA adducts. DNA damage can activate ATM (ataxia telangiectasia-mutated) and ATR (ATM-related), two apical DNA damage responsive protein kinases [2,42,43]. Upon activation, ATM and ATR may directly phosphorylate and activate p53. Alternatively, they may activate downstream protein kinases such as CHK1 and CHK2, which then phosphorylate p53 [2,42,43]. In renal cells and tissues, whether ATM and ATR are activated in response to cisplatin and involved in subsequent p53 activation is unclear. Our recent work indicates that ATM, but not ATR, is proteolytically cleaved and inactivated during cisplatin treatment of renal tubular cells [44]. In the current study, we showed that p53 is phosphorylated rapidly during cisplatin treatment and the phosphorylation occurs prior to p53 protein accumulation. This observation is consistent with the general understanding of p53 regulation, which involves multiple mechanisms at the transcriptional and post-transcriptional levels. Phosphorylation is an important post-transcriptional mechanism of p53 regulation, which leads to p53 stabilization and accumulation in cells. It is not very clear how phosphorylation stabilizes p53; nevertheless phosphorylation may prevent MDM2 binding and targeting p53 to degradation [40,41]. Certainly, further studies should investigate these DNA damage responsive pathways and their possible regulation by hydroxyl radicals during cisplatin nephrotoxicity.

It is important to recognize that in addition to ATM/ATR pathways, several other protein kinases have also been implicated in p53 phosphorylation and activation [40]. These include PKC, ERK, JNK, p38 and others. Interestingly, these protein kinases have also been shown to participate in cisplatin-induced renal cell injury and apoptosis. In primary cultures of rabbit proximal tubular cells, Nowak has shown that PKC-α and ERK1/2 mediate mitochondrial dysfunction and Na^+ transport and apoptosis [10]. In immortalized proximal tubular cells, Arany et al. have demonstrated a specific role of ERK (and not JNK or p38) in cisplatin-induced apoptosis [17]. The results are supported by recent work of Kim et al. [45]. On the other hand, Sheikh-Hamad et al. have suggested the involvement of JNK in tubular cell apoptosis by correlating the sites of apoptosis and JNK activation during cisplatin nephrotoxicity [15]. Recent work by Ramesh and Reeves further indicates that inhibition of p38 kinase ameliorates cisplatin nephrotoxicity in mice, suggesting a role of this MAP kinase in the development of tissue pathology under this experimental model [28]. Thus, while several protein kinases have been implicated in cisplatin-induced renal cell injury and nephrotoxicity, it is unclear how the signaling pathways are integrated to promote apoptosis. Conceivably, their regulation may depend on the experimental condition. Moreover, they may regulate distinct or overlapping

steps of apoptotic signaling. As p53 plays an important role in tubular cell apoptosis following cisplatin treatment [19–22], it would be interesting to speculate that these protein kinases may directly or indirectly regulate p53 and, as a result, activate the apoptotic cascade.

Despite the potential involvements of various protein kinases in cisplatin nephrotoxicity, our understanding of the signals leading to their activation is very limited. In this area, Ramesh and Reeves have demonstrated that the hydroxyl radical scavenger DMTU can attenuate p38 activation during cisplatin treatment. Importantly, this is accompanied by the amelioration of cisplatin nephrotoxicity [28]. In our study, DMTU blocks p53 activation, tubular cell apoptosis and tissue damage during cisplatin treatment, and preserves renal function. We speculate that cisplatin induces a rapid accumulation of hydroxyl radicals, leading to the activation of protein kinases (e.g. p38), which then phosphorylate and stabilize p53. p53 triggers apoptosis via transcription-dependent and -independent pathways. Apparently, this is a simplistic view of cisplatin injury, as the chemotherapy drug may have multiple molecular and structural targets within the cell, and p53 is only one of the injurious events that are activated during cisplatin nephrotoxicity.

Acknowledgements

We thank Dr. U. Hopferat Case Western Reserve University for the rat kidney proximal tubular cell (RPTC) line. We also thank Dr. J. Yu at University of Pittsburgh for the rabbit polyclonal anti-PUMA antibody. The study was supported in part by grants from National Institutes of Health and Department of Veterans Affairs of USA.

REFERENCES

1. Fuertesa MA, Castillab J, Alonsoa C, Perez JM. Cisplatin biochemical mechanism of action: from cytotoxicity to induction of cell death through interconnections between apoptotic and necrotic pathways. Curr Med Chem 2003;10(3):257–266. [PubMed: 12570712]
2. Siddik ZH. Cisplatin: mode of cytotoxic action and molecular basis of resistance. Oncogene 2003;22 (47):7265–7279. [PubMed: 14576837]
3. Arany I, Safirstein RL. Cisplatin nephrotoxicity. Semin Nephrol 2003;23(5):460–464. [PubMed: 13680535]
4. Taguchi T, Nazneen A, Abid MR, Razzaque MS. Cisplatin-associated nephrotoxicity and pathological events. Contrib Nephrol 2005;148:107–121. [PubMed: 15912030]
5. Lieberthal W, Triaca V, Levine J. Mechanisms of death induced by cisplatin in proximal tubular epithelial cells: apoptosis vs. necrosis. Am J Physiol 1996;270(4 Pt 2):F700–F708. [PubMed: 8967349]
6. Baliga R, Zhang Z, Baliga M, Ueda N, Shah SV. In vitro and in vivo evidence suggesting a role for iron in cisplatin-induced nephrotoxicity. Kidney Int 1998;53(2):394–401. [PubMed: 9461098]
7. Kaushal GP, Kaushal V, Hong X, Shah SV. Role and regulation of activation of caspases in cisplatin-induced injury to renal tubular epithelial cells. Kidney Int 2001;60(5):1726–1736. [PubMed: 11703590]
8. Liu H, Baliga R. Cytochrome P450 2E1 null mice provide novel protection against cisplatin-induced nephrotoxicity and apoptosis. Kidney Int 2003;63(5):1687–1696. [PubMed: 12675844]
9. Megyesi J, Safirstein RL, Price PM. Induction of p21WAF1/CIP1/SDI1 in kidney tubule cells affects the course of cisplatin-induced acute renal failure. J Clin Invest 1998;101(4):777–782. [PubMed: 9466972]
10. Nowak G. Protein kinase C-alpha and ERK1/2 mediate mitochondrial dysfunction, decreases in active Na+ transport, and cisplatin-induced apoptosis in renal cells. J Biol Chem 2002;277(45):43377–43388. [PubMed: 12218054]
11. Park MS, De Leon M, Devarajan P. Cisplatin induces apoptosis in LLC-PK1 cells via activation of mitochondrial pathways. J Am Soc Nephrol 2002;13(4):858–865. [PubMed: 11912244]
12. Ramesh G, Reeves WB. TNF-alpha mediates chemokine and cytokine expression and renal injury in cisplatin nephrotoxicity. J Clin Invest 2002;110(6):835–842. [PubMed: 12235115]

13. Tsuruya K, Ninomiya T, Tokumoto M, Hirakawa M, Masutani K, Taniguchi M, et al. Direct involvement of the receptor-mediated apoptotic pathways in cisplatin-induced renal tubular cell death. Kidney Int 2003;63(1):72–82. [PubMed: 12472770]

14. Shiraishi F, Curtis LM, Truong L, Poss K, Visner GA, Madsen K, et al. Heme oxygenase-1 gene ablation or expression modulates cisplatin-induced renal tubular apoptosis. Am J Physiol Renal Physiol 2000;278(5):F726–F736. [PubMed: 10807584]

15. Sheikh-Hamad D, Cacini W, Buckley AR, Isaac J, Truong LD, Tsao CC, et al. Cellular and molecular studies on cisplatin-induced apoptotic cell death in rat kidney. Arch Toxicol 2004;78(3):147–155. [PubMed: 14551673]

16. Li S, Basnakian A, Bhatt R, Megyesi J, Gokden N, Shah SV, et al. PPAR-alpha ligand ameliorates acute renal failure by reducing cisplatin-induced increased expression of renal endonuclease G. Am J Physiol Renal Physiol 2004;287(5):F990–F998. [PubMed: 15280156]

17. Arany I, Megyesi JK, Kaneto H, Price PM, Safirstein RL. Cisplatin-induced cell death is EGFR/src/ERK signaling dependent in mouse proximal tubule cells. Am J Physiol Renal Physiol 2004;287(3):F543–F549. [PubMed: 15149969]

18. Yu F, Megyesi J, Safirstein RL, Price PM. Identification of the functional domain of p21WAF1/CIP1 that protects from cisplatin cytotoxicity. Am J Physiol Renal Physiol 2005;289:F514–F520. [PubMed: 15840769]

19. Cummings BS, Schnellmann RG. Cisplatin-induced renal cell apoptosis: caspase 3-dependent and-independent pathways. J Pharmacol Exp Ther 2002;302(1):8–17. [PubMed: 12065694]

20. Jiang M, Yi X, Hsu S, Wang CY, Dong Z. Role of p53 in cisplatin-induced tubular cell apoptosis: dependence on p53 transcriptional activity. Am J Physiol Renal Physiol 2004;287(6):F1140–F1147. [PubMed: 15315938]

21. Seth R, Yang C, Kaushal V, Shah SV, Kaushal GP. p53-dependent caspase-2 activation in mitochondrial release of apoptosis-inducing factor and its role in renal tubular epithelial cell injury. J Biol Chem 2005;280(35):31230–31239. [PubMed: 15983031]

22. Jiang M, Wei Q, Wang J, Du C, Yu J, Zhang L, et al. Regulation of PUMA-alpha by p53 in cisplatin-induced renal cell apoptosis. Oncogene 2006;25:4056–4066. [PubMed: 16491117]

23. Baliga R, Ueda N, Walker PD, Shah SV. Oxidant mechanisms in toxic acute renal failure. Drug Metab Rev 1999;31(4):971–997. [PubMed: 10575556]

24. Nath KA, Norby SM. Reactive oxygen species and acute renal failure. Am J Med 2000;109(8):665–678. [PubMed: 11099687]

25. Martindale JL, Holbrook NJ. Cellular response to oxidative stress: signaling for suicide and survival. J Cell Physiol 2002;192(1):1–15. [PubMed: 12115731]

26. Baek SM, Kwon CH, Kim JH, Woo JS, Jung JS, Kim YK. Differential roles of hydrogen peroxide and hydroxyl radical in cisplatin-induced cell death in renal proximal tubular epithelial cells. J Lab Clin Med 2003;142(3):178–186. [PubMed: 14532906]

27. Matsushima H, Yonemura K, Ohishi K, Hishida A. The role of oxygen free radicals in cisplatin-induced acute renal failure in rats. J Lab Clin Med 1998;131(6):518–526. [PubMed: 9626987]

28. Ramesh G, Reeves WB. p38 MAP kinase inhibition ameliorates cisplatin nephrotoxicity in mice. Am J Physiol Renal Physiol 2005;289:F166–F174. [PubMed: 15701814]

29. Satoh M, Kashihara N, Fujimoto S, Horike H, Tokura T, Namikoshi T, et al. A novel free radical scavenger, edarabone, protects against cisplatin-induced acute renal damage in vitro and in vivo. J Pharmacol Exp Ther 2003;305(3):1183–1190. [PubMed: 12649298]

30. Sueishi K, Mishima K, Makino K, Itoh Y, Tsuruya K, Hirakata H, et al. Protection by a radical scavenger edaravone against cisplatin-induced nephrotoxicity in rats. Eur J Pharmacol 2002;451(2):203–208. [PubMed: 12231392]

31. Tsuruya K, Tokumoto M, Ninomiya T, Hirakawa M, Masutani K, Taniguchi M, et al. Antioxidant ameliorates cisplatin-induced renal tubular cell death through inhibition of death receptor-mediated pathways. Am J Physiol Renal Physiol 2003;285(2):F208–F218. [PubMed: 12684229]

32. Halliwell B, Grootveld M, Gutteridge JM. Methods for the measurement of hydroxyl radicals in biomedical systems: deoxyribose degradation and aromatic hydroxylation. Methods Biochem Anal 1988;33:59–90. [PubMed: 2833681]

33. Wang J, Wei Q, Wang CY, Hill WD, Hess DC, Dong Z. Minocycline up-regulates Bcl-2 and protects against cell death in the mitochondria. J Biol Chem 2004;279(19):19948–19954. [PubMed: 15004018]
34. Dong Z, Wang J. Hypoxia selection of death-resistant cells: a role for Bcl-XL. J Biol Chem 2004;279 (10):9215–9221. [PubMed: 14676192]
35. Gottlieb RA, Granville DJ. Analyzing mitochondrial changes during apoptosis. Methods 2002;26(4): 341–347. [PubMed: 12054925]
36. Dong Z, Wang JZ, Yu F, Venkatachalam MA. Apoptosis-resistance of hypoxic cells: multiple factors involved and a role for IAP-2. Am J Pathol 2003;163(2):663–671. [PubMed: 12875985]
37. Wei Q, Wang MH, Dong Z. Differential gender differences in ischemic and nephrotoxic acute renal failure. Am J Nephrol 2005;25(5):491–499. [PubMed: 16155358]
38. Wei Q, Yin XM, Wang MH, Dong Z. Bid deficiency ameliorates ischemic renal failure and delays animal death in C57BL/6 mice. Am J Physiol Renal Physiol 2006;290(1):F35–F42. [PubMed: 16106037]
39. Ramesh G, Reeves WB. TNFR2-mediated apoptosis and necrosis in cisplatin-induced acute renal failure. Am J Physiol Renal Physiol 2003;285(4):F610–F618. [PubMed: 12865254]
40. Bode AM, Dong Z. Post-translational modification of p53 in tumorigenesis. Nat Rev Cancer 2004;4 (10):793–805. [PubMed: 15510160]
41. Vousden KH, Lu X. Live or let die: the cell's response to p53. Nat Rev Cancer 2002;2(8):594–604. [PubMed: 12154352]
42. Norbury CJ, Zhivotovsky B. DNA damage-induced apoptosis. Oncogene 2004;23(16):2797–2808. [PubMed: 15077143]
43. Shiloh Y. ATM and related protein kinases: safeguarding genome integrity. Nat Rev Cancer 2003;3 (3):155–168. [PubMed: 12612651]
44. Wang J, Pabla N, Wang CY, Wang W, Schoenlein PV, Dong Z. Caspase-mediated cleavage of ATM during cisplatin-induced tubular cell apoptosis: inactivation of its kinase activity toward p53. Am J Physiol Renal Physiol 2006;291(6):F1300–F1307. [PubMed: 16849690]
45. Kim YK, Kim HJ, Kwon CH, Kim JH, Woo JS, Jung JS, et al. Role of ERK activation in cisplatin-induced apoptosis in OK renal epithelial cells. J Appl Toxicol 2005;25(5):374–382. [PubMed: 16013042]

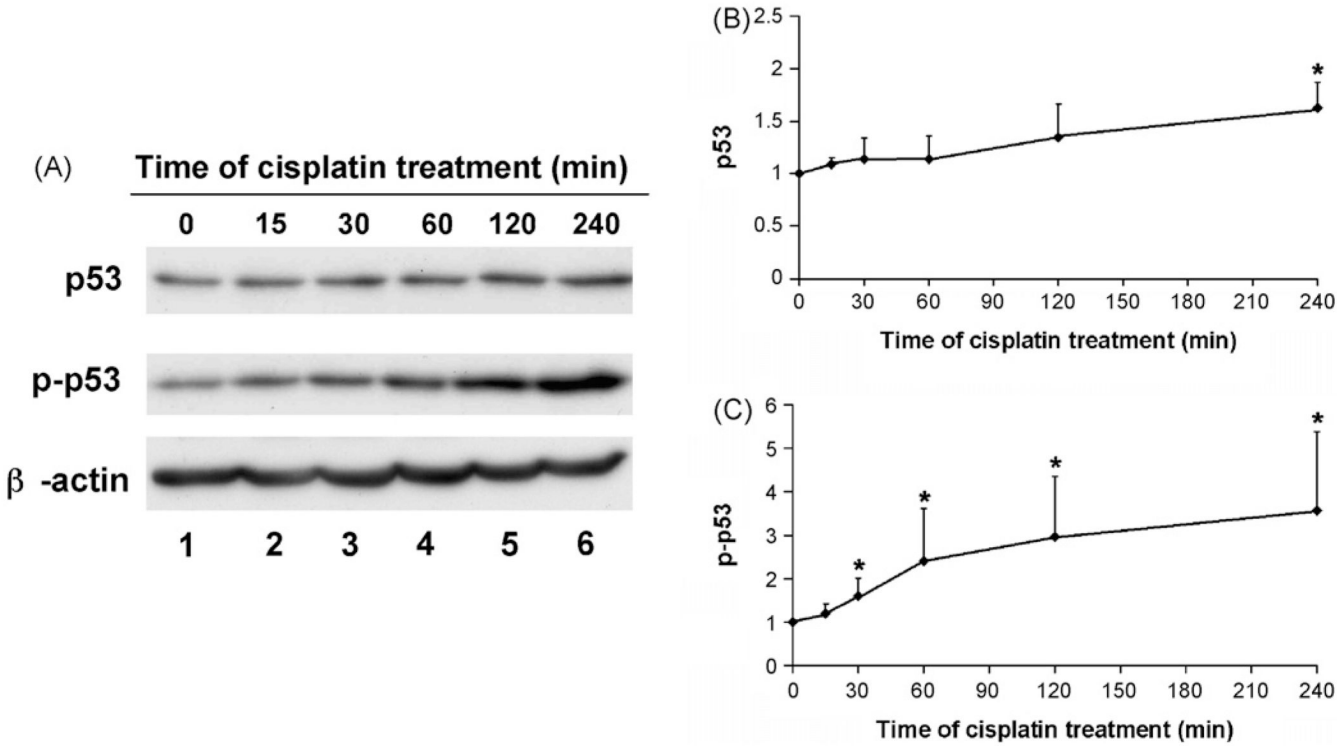

Fig. 1.

Early p53 activation during cisplatin treatment. RPTC cells were incubated with 20 μM cisplatin for 0–240 min. Whole cell lysate was collected for immunoblot analysis of total p53 and phosphorylated p53 (p-p53). The blots were then reprobed for β-actin to monitor protein loading and transferring. (A) Representative immunoblots. (B) Densitometry of p53. (C) Densitometry of p-p53. For densitometric analysis, the p53 or p-p53 signals of control cells was arbitrarily set as 1 in each blot, and the signals of experimental conditions in the same blot were normalized with the control to show their p53 or p-p53 levels. The results were from at least three immunoblots of separate experiments. Data are expressed as mean ± S.D. ($n \geq 3$). *Statistically significantly different from the control.

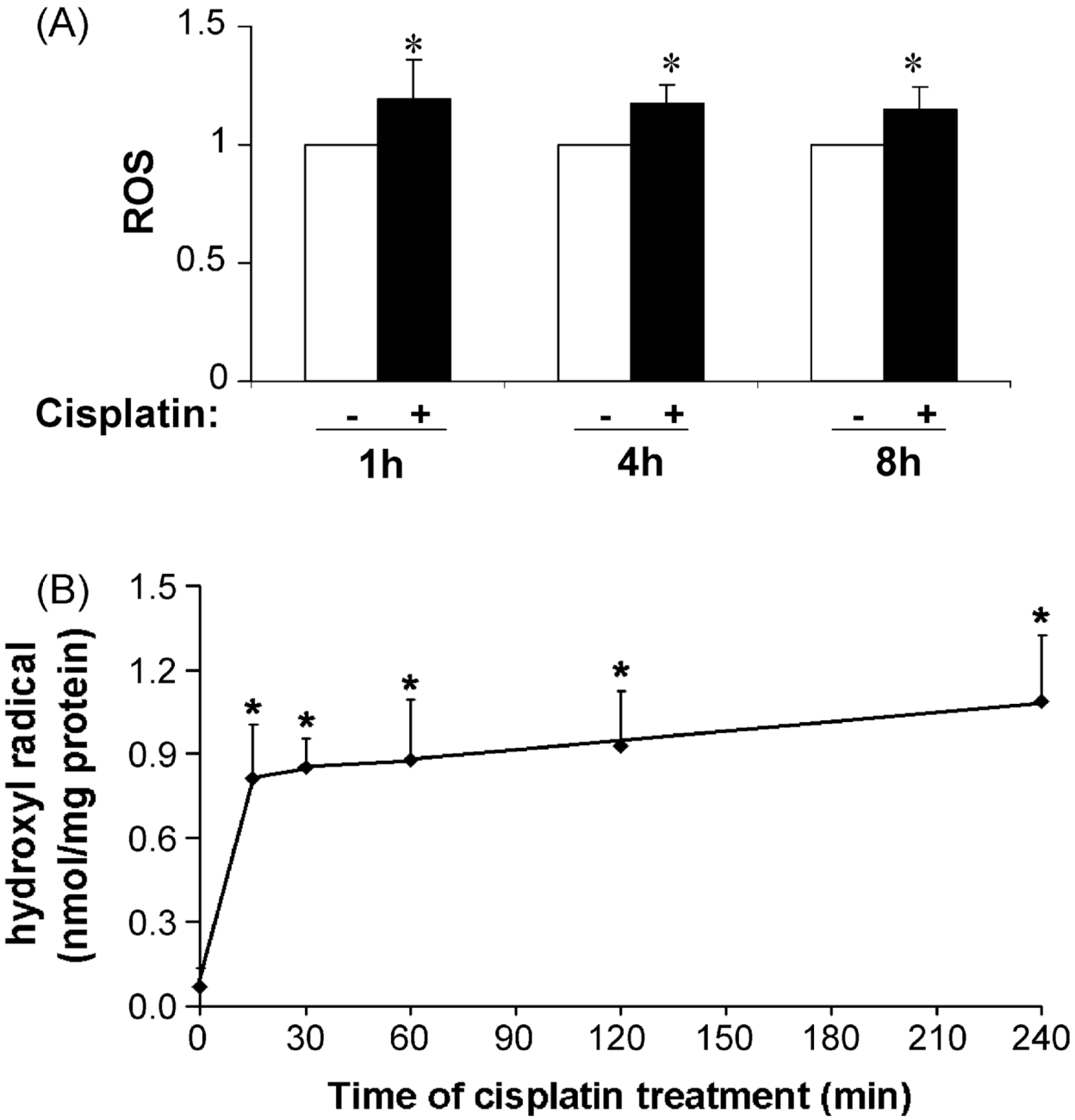

Fig. 2.

ROS and hydroxyl radical accumulation during cisplatin treatment. RPTC cells were incubated with 20 μM cisplatin for indicated time. (A) ROS accumulation. ROS was measured using the fluoregenic dye DCF as described in Section 2. The fluorescence signals of the experimental samples were normalized with the values of the control, which was arbitrarily set as 1. (B) Hydroxyl radical accumulation. Hydroxyl radicals were measured by the deoxyribose degradation assay as detailed in Section 2. Data are expressed as mean ± S.D. (n = 4). *Statistically significantly different from the control group without cisplatin treatment. The results demonstrate a marginal increase of total ROS and a drastic accumulation of hydroxyl radicals during cisplatin treatment.

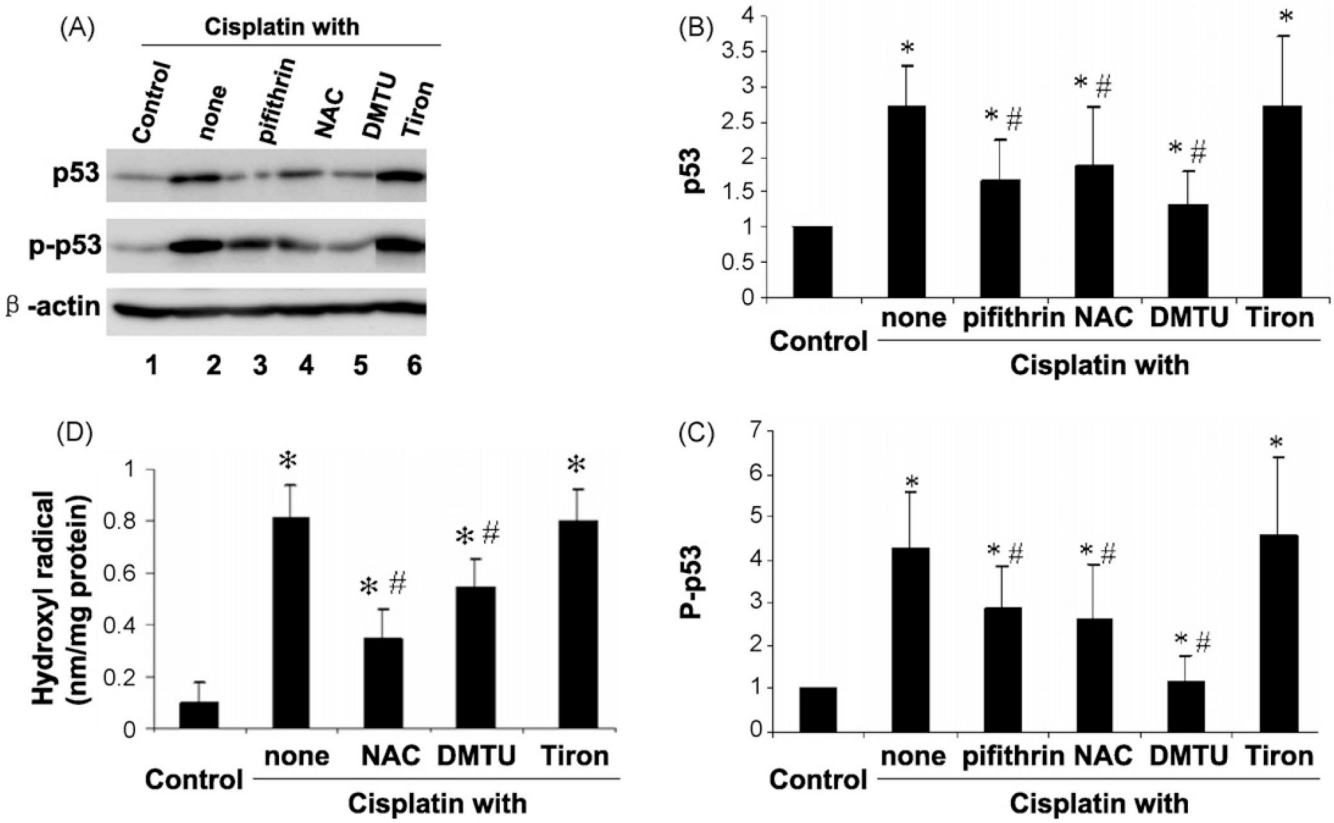

Fig. 3.

Effects of ROS scavengers on p53 activation and hydroxyl radical formation during cisplatin treatment. (A–C) RTPC cells were incubated with 20 μM cisplatin for 16 h in the absence or presence of 20 μM pifithrin-α, 10 mM *N*-acetyl-cysteine (NAC), 10 mM DMTU, or 10 mM Tiron. Whole cell lysate was collected for immunoblot analysis of p53 and phospho-p53. The blots were also reprobed for β-actin to monitor protein loading and transferring. (A) Representative immunoblots. (B) Densitometry of p53. (C) Densitometry of p-p53. For densitometric analysis, the p53 or p-p53 signals of control cells was arbitrarily set as 1 in each blot, and the signals of experimental conditions in the same blot were normalized with the control to show their p53 or p-p53 levels. The results were from at least three immunoblots of separate experiments. (D) RPTC cells were incubated with 20 μM cisplatin for 1 h in the absence or presence of 10 mM NAC, 10 mM DMTU, 10 mM mannitol, 2 mM benzoate, or 10 mM Tiron. Hydroxyl radicals were measured by the deoxyribose degradation assay as detailed in Section 2. Data are expressed as mean ± S.D. ($n \geq 3$). *Statistically significantly different from the control; #significantly different from the cisplatin-only group. The results show that p53 activation during cisplatin treatment is suppressed by the general antioxidant NAC and the hydroxyl radical scavenger DMTU.

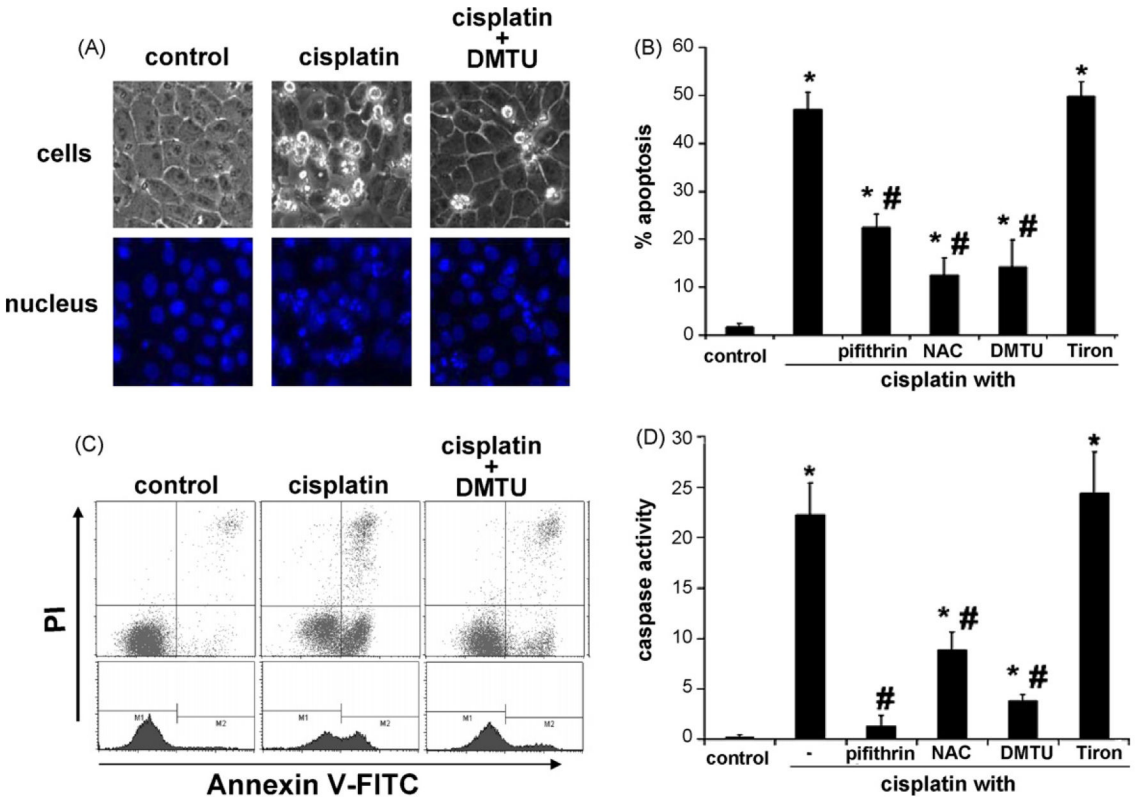

Fig. 4.

Effects of NAC and DMTU on tubular cell apoptosis during cisplatin treatment. RPTC cells were incubated with 20 μM cisplatin for 16 h in the absence or presence of 10 mM NAC, 10 mM DMTU, or 10 mM Tiron. (A) Representative images of cell morphology. At the end of incubation, cells were stained with Hoechst 33342. Cellular and nuclear morphology was recorded by phase contrast and fluorescence microscopy, respectively. (B) Percentage of apoptosis. Apoptotic cells were examined by morphological methods and counted to assess the percentage of apoptosis. (C) Representative flow cytometric analysis of Annexin V-FITC and PI staining. (D) Caspase activity. Cell lysate was collected for enzymatic assay of caspase activity as described in Section 2. Data are expressed as mean ± S.D. (n = 4). *Statistically significantly different from the control group; #significantly different from the cisplatin-only group. The results show that NAC and DMTU suppressed cisplatin-induced caspase activation and apoptosis.

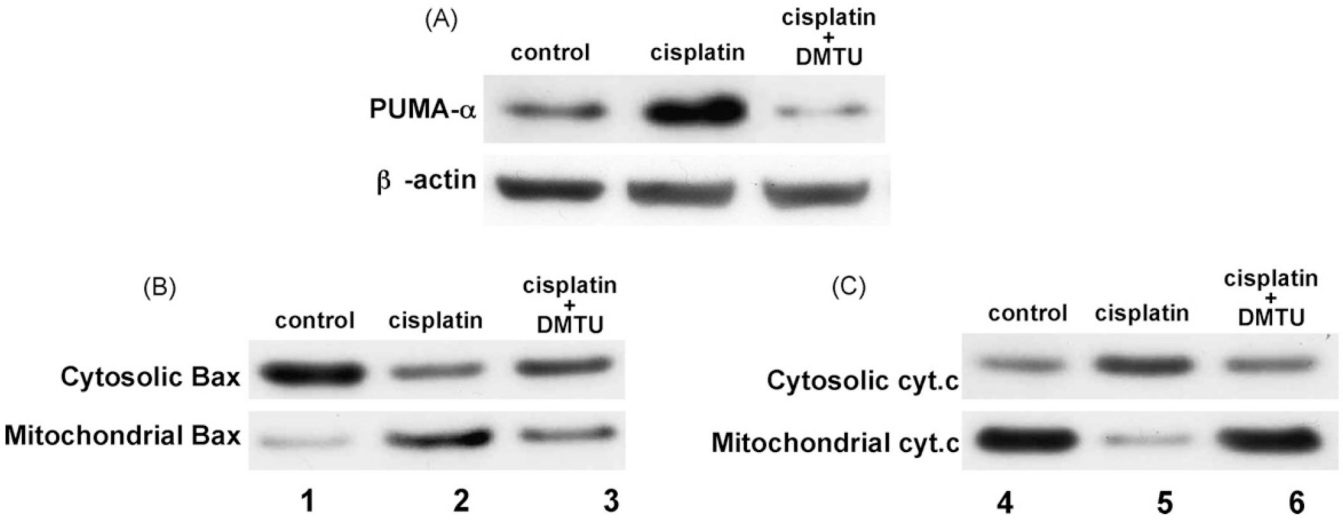

Fig. 5.

Effects of DMTU on PUMA-α induction, Bax translocation, and cytochrome c translocation during cisplatin treatment. RPTC cells were incubated with 20 μM cisplatin for 16 h in the absence or presence of 10 mM DMTU. (A) PUMA-α induction. Whole cell lysate was collected for immunoblot analysis of PUMA-α. The blots were reprobed for β-actin to monitor protein loading and transferring. (B) Bax translocation. The cells were fractionated into the cytosolic and mitochondrial fractions for immunoblot analysis of Bax. (C) Cytochrome c release. The cells were fractionated into the cytosolic and mitochondrial fractions for immunoblot analysis of cytochrome c. Shown in this figure are representative blots of three separate experiments. The results show that DMTU attenuates PUMA-α induction and Bax translocation and cytochrome c release during cisplatin treatment of renal tubular cells.

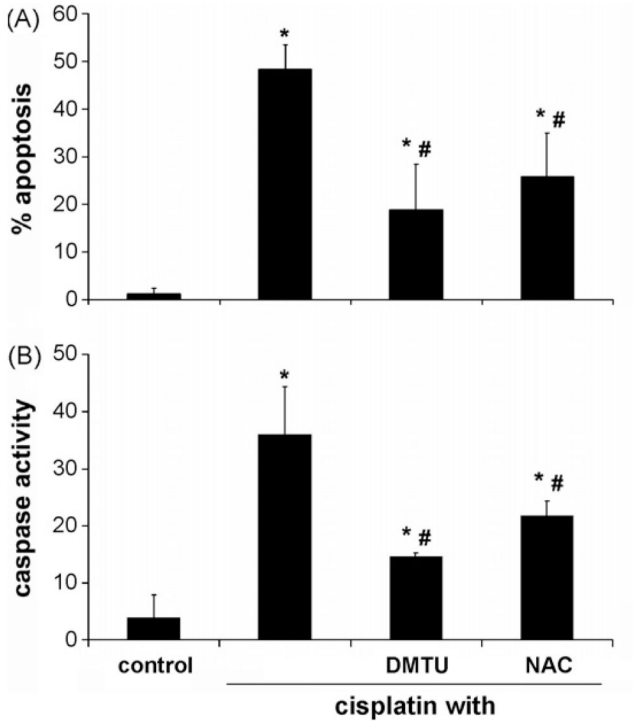

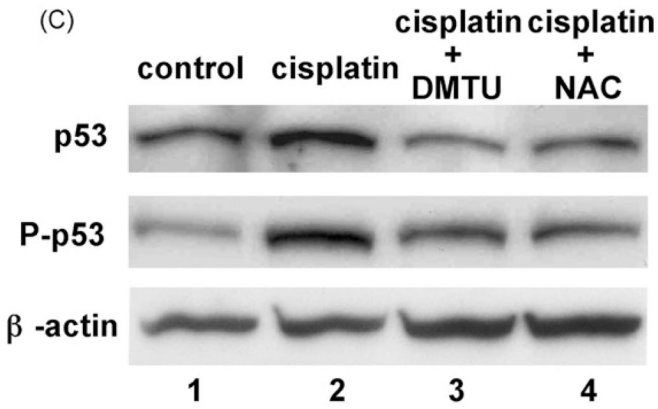

Fig. 6.

DMTU and NAC added after cisplatin treatment suppresses p53 activation and apoptosis in renal tubular cells. RPTC cells were incubated with 20 μM cisplatin for 2 h. Then cisplatin was removed for further 22 h of incubation in the presence or absence of 5 mM DMTU or 0.5 mM NAC. (A) %Apoptosis. (B) Caspase activity. Data are expressed as means ± S.D. (n = 6). *Statistically significantly different from the control group; #significantly different from the cisplatin-only group. (C) Representative blots for p53 and phospho-p53. Whole cell lysates were examined by immunoblot analysis.

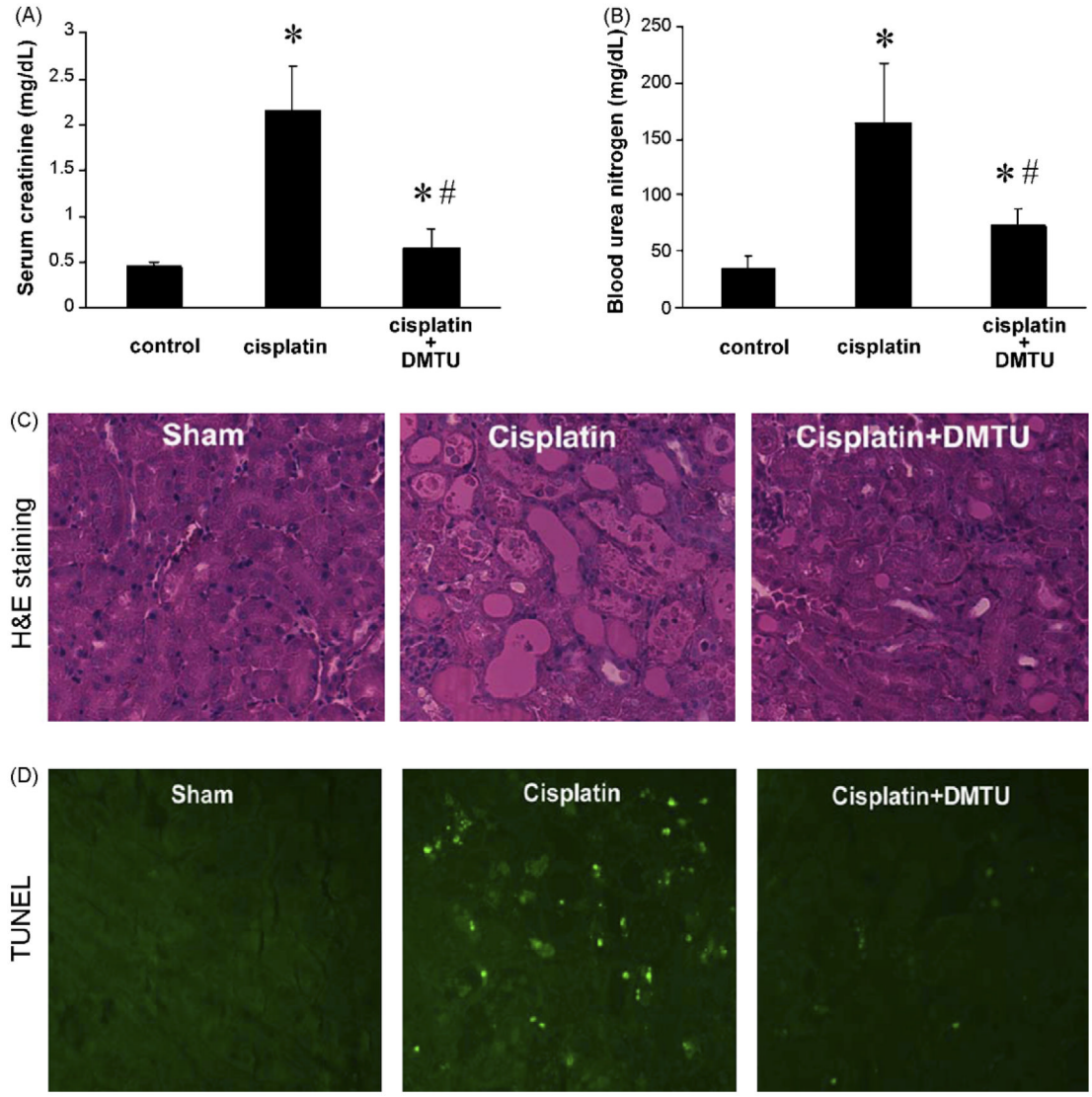

Fig. 7.

Effects of DMTU on renal function during cisplatin treatment *in vivo*. C57BL/6 mice (male, 8–10 weeks old) were divided into three groups. The cisplatin group was treated with a single dose of cisplatin (i.p., 30 mg/kg) for 3 days. The cisplatin + DMTU group was given 100 mg/kg DMTU 30 min prior to cisplatin injection, and then DMTU was given daily post-cisplatin injection. The control group was injected with vehicle solution. (A) Serum creatinine. (B) Blood urea nitrogen. Blood samples were collected to obtain serum for the measurement of creatinine and BUN, as described in Section 2. Data are expressed as mean ± S.D. (n = 5). *Statistically significantly different from the control group; #significantly different from the cisplatin-only group. The results show renoprotective effects of DMTU against cisplatin-induced nephrotoxicity.

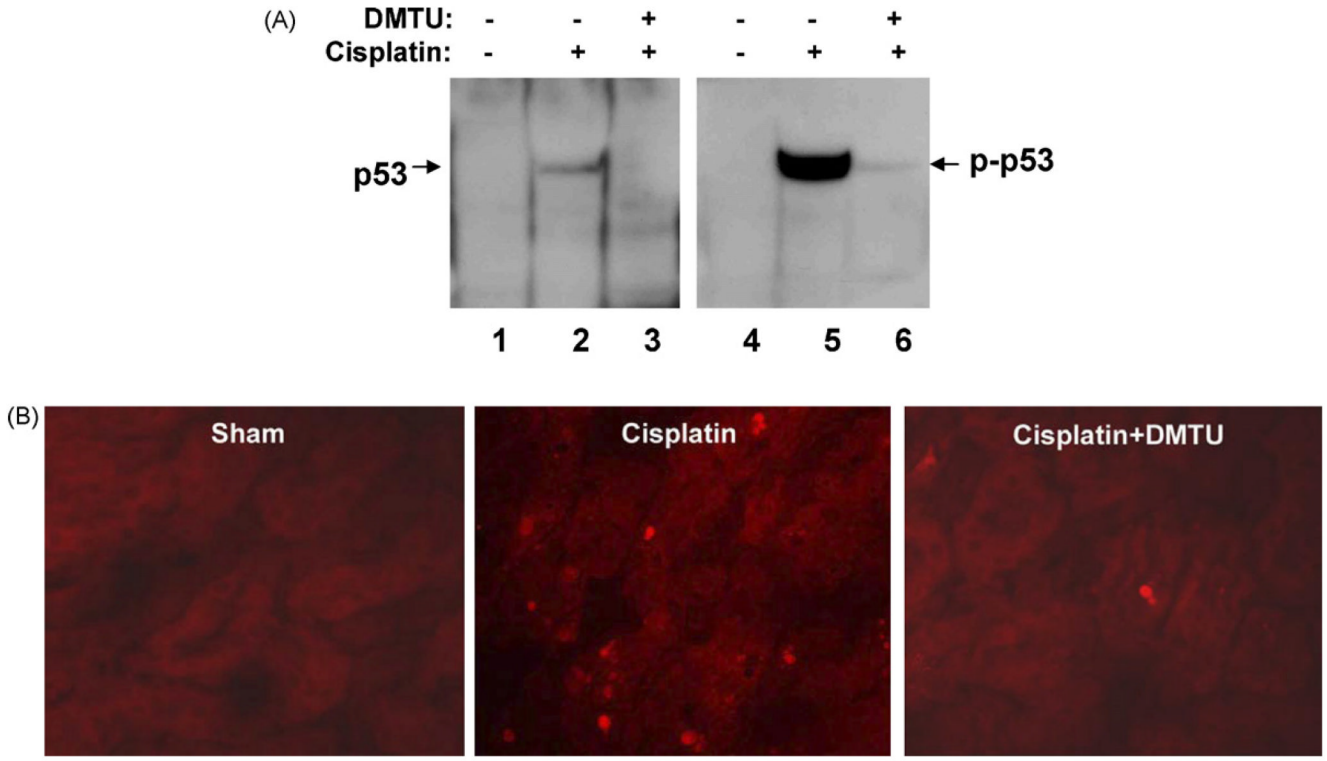

Fig. 8.

Effects of DMTU on p53 activation *in vivo* during cisplatin treatment. C57BL/6 mice (male, 8–10 weeks old) were divided into three groups for experiment: control, cisplatin, and cisplatin + DMTU. The cisplatin group was treated with a single dose of cisplatin (i.p., 30 mg/kg) for 3 days. The cisplatin + DMTU group was given 100 mg/kg DMTU 30 min prior to cisplatin injection, and then DMTU was given daily post-cisplatin injection. The control group was injected with vehicle solution. At the end of experiment, renal tissues were collected for immunoblot and immunofluorescence analysis of p53. (A) Immunoblot analysis of p53 and phospho-p53. Renal cortical tissues were homogenized and extracted with 2% SDS for immunoblot analysis of p53 and phospho-p53. The blots were reprobed for β-actin to monitor comparable protein loading and transferring in each lane (not shown). (B) Immunofluorescence of p53. Renal tissues were processed for immunofluorescence as described in Section 2. Shown in the figure are representative results of four animals in each group. The results show that p53 activation during cisplatin treatment is ameliorated by DMTU.